Energy Stable Model Order Reduction for the Allen-Cahn Equation

Bülent Karasözen
joint work with Murat Uzunca & Tugba Küçükseyhan

Institute of Applied Mathematics & Department of Mathematics, METU, Ankara

MODRED 2017, 11-13 January

Outline

Evolutionary PDEs

$$u_t = \mathscr{D}\frac{\delta \mathscr{H}}{\delta u}, \quad (x,t) \in \Omega \times (0,T],$$

$$\mathscr{H} = \int_\Omega (H(x; u, u_x, u_{xx}, \dots) dx$$

Variational derivative:

$$\frac{\delta \mathscr{H}}{\delta u} = \frac{\partial H}{\partial u} - \partial_x \left(\frac{\partial H}{\partial u_x} \right) - \partial_x^2 \left(\frac{\partial H}{\partial u_{xx}} \right)$$

Conservative PDEs

$\mathscr{D} = \mathscr{S}$ constant skew-adjoint operator in $\mathscr{B} = L_2(\Omega)$.

$$\int_{\Omega} u \mathscr{S} u dx = 0, \quad \forall \mathscr{B}$$

$\mathscr{H}$ Hamiltonian (energy) conserving system

$$\frac{d\mathscr{H}}{dt} = \int_{\Omega} \frac{\delta \mathscr{H}}{\delta u} \mathscr{S} \frac{\delta \mathscr{H}}{\delta u} dx = 0$$

Nonlinear Schrödinder (NLS) equation

$$\frac{\partial}{\partial t} \begin{pmatrix} u \\ u^* \end{pmatrix} = \begin{pmatrix} 0 & i \\ -i & 0 \end{pmatrix} \begin{pmatrix} \frac{\delta \mathscr{H}}{\delta u} \\ \frac{\delta \mathscr{H}}{\delta u} \end{pmatrix}$$

$$\mathscr{H} = \int_{\Omega} \left(-|\nabla u|^2 + \frac{\gamma}{2} |u|^4 \right) dx, \quad \mathscr{S} = \begin{pmatrix} 0 & i \\ -i & 0 \end{pmatrix}$$

Korteweg de Vries equation, Sine-Gordon equation, Maxwell equation

Dissipative PDEs

$\mathscr{D} = \mathscr{N}$ constant negative (semi) definite operator

$$\int_\Omega u\mathscr{N}u dx \leq 0, \quad \forall \mathscr{B}$$

$\mathscr{H}$ Lyapunov function, energy dissipating system

$$\dot{\mathscr{H}} = \int_\Omega \frac{\delta\mathscr{H}}{\delta u}\mathscr{N}\frac{\delta\mathscr{H}}{\delta u}dx \leq 0$$

Allen-Cahn equation

$$\frac{\partial u}{\partial t} = \varepsilon\Delta u + u - u^3$$

$$\mathscr{H} = \int_\Omega \left(\frac{\varepsilon}{2}|\nabla u|^2 - \frac{1}{2}u^2 + \frac{1}{4}u^4\right) dx, \quad \mathscr{N} = -1$$

Energy is monotonically decreasing

$\mathscr{H}(u(t_n)) < \mathscr{H}(u(t_m)), \quad \forall t_n > t_m$

Cahn-Hilliard Equation, Ginzburg-Landau equation

Fitzhugh-Nagumo equation

$$\begin{aligned} \tau_1 u_t &= d_1 \Delta u + f(u,v) \\ \tau_2 v_t &= d_2 \Delta v + g(u,v) \end{aligned}$$

Skew-gradient structure

$$\frac{\partial}{\partial v}\left(\frac{f(u,v)}{\tau_1}\right) = -\frac{\partial}{\partial u}\left(\frac{g(u,v)}{\tau_2}\right).$$

$$E(u,v) = \int_\Omega \left(\frac{d_1}{2}|\nabla u|^2 - \frac{d_2}{2}|\nabla v|^2 + F(u,v)\right) \mathrm{d}x$$

with the potential function

$$F(u,v) = -\frac{u^4}{4} + \frac{(1+\beta)u^3}{3} - \frac{\beta u^2}{2} - uv + \frac{\gamma v^2}{2} - \varepsilon v$$

Symmetric interior penalty Galerkin (SIPG)

- $\xi_h = \{K\}$ is a partition of the computational domain Ω into a family of triangles.
- $\mathbb{P}_k(K)$ is the space of polynomials of order k on the element K.

The finite dimensional solution and test function space

$$W_h = W_h(\xi_h) = \left\{ w \in L^2(\Omega) : w|_K \in \mathbb{P}_k(K),\ \forall K \in \xi_h \right\},$$

where $w \in W_h$ is *discontinuous* along the inter-element boundaries.

B. Rivière. Discontinuous Galerkin methods for solving elliptic and parabolic equations, Theory and implementation. SIAM, 2008.

- The jump and average operators of a function $w \in W_h$ on an interior edge $e \subset \partial K_i \cap K_j$:

$$[\![w]\!] := w|_{K_i}\mathbf{n}_{K_i} + w|_{K_j}\mathbf{n}_{K_j}\ , \quad \{\{w\}\} := \frac{1}{2}(w|_{K_i} + w|_{K_j}),$$

with $[\![w]\!] := w|_K\mathbf{n}$ and $\{\{w\}\} := w|_K$ on a boundary edge $e \subset \partial\Omega$.

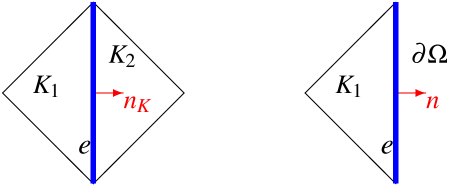

- The sets of inflow and outflow edges:

$$\begin{aligned} \Gamma^- &= \{\mathbf{z} \in \partial\Omega : \mathbf{b}(v)\cdot\mathbf{n}(v,x) < 0\}\ , \qquad \Gamma^+ = \partial\Omega \setminus \Gamma^-, \\ \partial K^- &= \{\mathbf{z} \in \partial K : \mathbf{b}(v)\cdot\mathbf{n}_K(v,x) < 0\}\ , \quad \partial K^+ = \partial K \setminus \partial K^-, \end{aligned}$$

where $\mathbf{n}_K$ is the outward unit vector on ∂K.

Symmetric interior penalty Galerkin (SIPG) discretization

Symmetric interior penalty Galerkin (SIPG) discretization

$$(\partial_t u_h(\mu), \upsilon_h)_\Omega + a_h(\mu; u_h(\mu), \upsilon_h) + (f(u_h(\mu);\mu), \upsilon_h)_\Omega = 0, \ \forall \upsilon_h \in V_h,$$

with the SIPG bilinear form

$$\begin{aligned} a_h(\mu; u, \upsilon) = & \sum_{K \in \mathscr{T}_h} \int_K \varepsilon \nabla u \cdot \nabla \upsilon - \sum_{E \in E_h^0} \int_E \{\varepsilon \nabla u\} [\upsilon] ds \\ & - \sum_{E \in E_h^0} \int_E \{\varepsilon \nabla \upsilon\} [u] + \sum_{E \in E_h^0} \frac{\sigma \varepsilon}{h_E} \int_E [u][\upsilon] ds, \end{aligned}$$

Full order model

$$u_h(x,t) = \sum_{i=1}^{n_e} \sum_{j=1}^{n_q} u_j^i(t)\varphi_j^i(x)$$

$$\boldsymbol{u} \quad := \boldsymbol{u}(t) = (u_1^1(t), u_2^1(t), \ldots, u_{n_q}^{n_e}(t))^T := (u_1(t), u_2(t), \ldots, u_{\mathcal{N}}(t))^T$$
$$\boldsymbol{\varphi} \quad := \boldsymbol{\varphi}(x) = (\varphi_1^1(x), \varphi_2^1(x), \ldots, \varphi_{n_q}^{n_e}(x))^T := (\varphi_1(x), \varphi_2(x), \ldots, \varphi_{\mathcal{N}}(x))^T$$

$\mathcal{N} = n_e \times n_q$ the dG degrees of freedom (DoFs)

$$\boldsymbol{M}\boldsymbol{u}_t = -\boldsymbol{A}\boldsymbol{u} - \boldsymbol{f}(\boldsymbol{u})$$

$\boldsymbol{M} \in \mathbb{R}^{\mathcal{N}\times\mathcal{N}}$ is the mass matrix
$\boldsymbol{A} \in \mathbb{R}^{\mathcal{N}\times\mathcal{N}}$ is the stiffness matrix

Average vector filed method

Energy stable (conserving or dissipating) average vector field (AVF) method for ODEs $\dot{y} = \boldsymbol{f}(u)$

$$\boldsymbol{u}_n = \boldsymbol{u}_{n-1} + \Delta t \int_0^1 \boldsymbol{f}(\tau \boldsymbol{u}_n + (1-\tau)\boldsymbol{u}_{n-1}) d\tau.$$

$$\boldsymbol{M}\boldsymbol{u}^{n+1} = \boldsymbol{M}\boldsymbol{u}^n - \frac{\Delta t}{2}\boldsymbol{A}(\boldsymbol{u}^{n+1} + \boldsymbol{u}^n) - \Delta t \int_0^1 \boldsymbol{f}(\tau \boldsymbol{u}^{n+1} + (1-\tau)\boldsymbol{u}^n) d\tau$$

The nonlinear function is approximated by symmetric Gauss-Legendre quadrature $\sum_{i=1}^s b_i = \frac{1}{2}$

$$\boldsymbol{f}(\tau \boldsymbol{u}^{n+1} + (1-\tau)\boldsymbol{u}^n) d\tau \approx \sum_{i=1}^s b_i f(c_i u^{n+1} + (1-c_i)u^n)$$

AVF method coincides with the mid-point rule for quadratic $\boldsymbol{f}(\boldsymbol{u})$.

Celledoni, E., Grimm, V., McLachlan, R., McLaren, D., ONeale, D., Owren, B., Quispel, G.: Preserving energy resp. dissipation in numerical PDEs using the average vector field method. Journal of Computational Physics 231,

Energy stability of the full order model

The SIPG discretized energy function of the continuous energy

$$\mathcal{E}_h(u_h^n) = \frac{\varepsilon}{2}\|\nabla u_h^n\|^2_{L^2(\Omega)} + (F(u_h^n),1)_\Omega + \sum_{E\in E_h^0}\left(-(\{\varepsilon\nabla u_h^n\},[u_h^n])_E + \frac{\sigma\varepsilon}{2h_E}([u_h^n],[u_h^n])_E\right),$$

$$\mathcal{E}_h(u_h^{n+1}) - \mathcal{E}_h(u_h^n) = -\frac{1}{\Delta t}\|u_h^{n+1} - u_h^n\|^2_{L^2(\Omega)} \leq 0,$$

For Allen-Cahn equation:

$$\mathcal{E}_h(u_h^{n+1}) \leq \mathcal{E}_h(u_h^n)$$

For NLS equation:

$$\mathcal{E}_h(u_h^n) = \mathcal{E}_h(u_h^0)$$

POD

M-orthogonal reduced basis functions $\{\psi_{w,i}\}$, $i = 1, 2, \ldots, k$

$$\min_{\psi_{w,1},\ldots,\psi_{w,k}} \frac{1}{J}\sum_{j=1}^{J}\left\| w^j - \sum_{i=1}^{k}(w^j, \psi_{w,i})_{L^2(\Omega)}\psi_{w,i}\right\|_{L^2(\Omega)}^2$$

subject to $(\psi_{w,i}, \psi_{w,j})_{L^2(\Omega)} = \Psi_{w,\cdot,i}^T M \Psi_{w,\cdot,j} = \delta_{ij}\ ,\ 1 \le i, j \le k,$

The minimization problem is equivalent to the eigenvalue problem

$$\mathscr{U}\mathscr{U}^T M \Psi_{u,\cdot,i} = \sigma_{u,i}^2 \Psi_{u,\cdot,i} \quad i = 1, 2, \ldots, k$$

for $\Psi_{u,\cdot,i}$ the coefficient vectors of the POD basis functions $\psi_{u,i}$.
Selection of POD modes: energy criteria

$$\mathscr{E} = \frac{\sum_{i=1}^{l}\sigma_i^2}{\sum_{i=1}^{d}\sigma_i^2}$$

Reduced order model

The ROM solution $u_{h,r}(x,t)$ of dimension $N \ll \mathcal{N}$ by POD

$$u_h(x,t) \approx u_{h,r}(x,t) = \sum_{i=1}^{N} u_{i,r}(t)\psi_i(x), \qquad (\psi_i(x), \psi_j(x))_\Omega = \delta_{ij},$$

SIPG weak formulation for ROM

$$(\partial_t u_{h,r}, \upsilon_{h,r})_\Omega + a_h(u_{h,r}, \upsilon_{h,r}) + (f(u_{h,r}), \upsilon_{h,r})_\Omega = 0, \forall \upsilon_{h,r} \in V_{h,r}$$

$$\psi_i(x) = \sum_{j=1}^{\mathcal{N}} \Psi_{j,i}\varphi_j(x), \qquad \Psi_{\cdot,i}^T M \Psi_{\cdot,j} = \delta_{ij}.$$

$\boldsymbol{\Psi} = [\Psi_{\cdot,1}, \ldots, \Psi_{\cdot,N}] \in \mathbb{R}^{\mathcal{N} \times N}$.
$\boldsymbol{u} = \boldsymbol{\Psi}\boldsymbol{u}_r$. The reduced semi-discrete ODE system:

$$\partial_t \boldsymbol{u}_r + \boldsymbol{A}_r \boldsymbol{u}_r + \boldsymbol{f}_r(\boldsymbol{u}_r) = \boldsymbol{0},$$

Reduced stiffness matrix $\rightarrow$ $\boldsymbol{A}_r = \boldsymbol{\Psi}^T \boldsymbol{A} \boldsymbol{\Psi}$
Reduced non-linear vector $\rightarrow$ $\boldsymbol{f}_r(\boldsymbol{u}_r) = \boldsymbol{\Psi}^T \boldsymbol{f}(\boldsymbol{\Psi}\boldsymbol{u}_r)$.

Discrete empirical interpolation (DEIM)

- Computation of $\boldsymbol{f}_r(\boldsymbol{u}_r) = \boldsymbol{\Psi}^T \boldsymbol{f}(\boldsymbol{\Psi}\boldsymbol{u}_r) \in \mathbb{R}^N$ depends on the dimension $\mathcal{N}$ of the full system

$$\boldsymbol{f}_r(\boldsymbol{u}_r) = \underbrace{\boldsymbol{\Psi}^T}_{N\times\mathcal{N}} \underbrace{\boldsymbol{f}(\boldsymbol{\Psi}\boldsymbol{u}_r(t))}_{\mathcal{N}\times 1}$$

- Use an approximation

$$\boldsymbol{f} \approx W\mathbf{s}, \quad W \in \mathbb{R}^{\mathcal{N}\times m}, \mathbf{c} \in \mathbb{R}^m$$

- It is over determined. Find a projection P such that:

$$P = [\mathbf{e}_{\wp_1}, \ldots, \mathbf{e}_{\wp_m}] \in \mathbb{R}^{\mathcal{N}\times m}$$

with $\mathbf{e}_{\wp_i}$ is the $\wp_i$-th column of the identity matrix $I \in \mathbb{R}^{\mathcal{N}\times\mathcal{N}}$

DEIM Algorithm

To find permutation matrix P and indices $\wp = [\wp_1, \ldots, \wp_m]^T$

Algorithm 1 The DEIM Algorithm

INPUT: $\{W_i\}_{i=1}^m \subset \mathbb{R}^{\mathcal{N}}$
OUTPUT: $\vec{\wp} = [\wp_1, ..., \wp_m]^T \in \mathbb{R}^m,\ P \in \mathbb{R}^{\mathcal{N} \times m}$
$[|\rho|, \wp_1] = \max\{|W_1|\}$
$W = [W_1], P = [\mathbf{e}_{\wp_1}], \vec{\wp} = [\wp_1]$
for $i = 2$ to m **do**
  Solve $(P^T W)\mathbf{c} = P^T W_i$ for $\mathbf{c}$
  $\mathbf{r} = W_i - W\mathbf{c}$
  $[|\rho|, \wp_i] = \max\{|\mathbf{r}|\}$
  $W \leftarrow [W\ W_i], P \leftarrow [P\ \mathbf{e}_{\wp_i}], \vec{\wp} \leftarrow \begin{bmatrix} \vec{\wp} \\ \wp_i \end{bmatrix}$
end for

S. Chaturantabut and D.C. Sorensen, *Nonlinear model reduction via discrete empirical interpolation* , SIAM Journal on Scientific Computing 32 (5), 2737–2764, 2010.

Finding the basis W

To find (POD) basis functions $W = [W_1, \dots, W_m] \in \mathbb{R}^{\mathcal{N} \times m}$:

- Set the snapshot matrix

$$\mathscr{F} := [\boldsymbol{f}^1, \dots, \boldsymbol{f}^J] \in \mathbb{R}^{\mathcal{N} \times J}, \text{ where } \boldsymbol{f}^i := \boldsymbol{f}(\boldsymbol{\Psi} \boldsymbol{u}_r(t_i))$$

- Set $\{W_i\}_{i=1}^m$ as the first $m \ll \mathcal{N}$ left singular vectors $\{\boldsymbol{W}_i\}_{i=1}^m$ through the SVD of $\mathscr{F}$

$$\mathscr{F} = \boldsymbol{W} \Sigma \boldsymbol{Z}^T$$

Approximating the nonlinearity

After finding P and $\wp = [\wp_1, \dots, \wp_m]^T$

$$
\begin{aligned}
P^T \boldsymbol{f} = (P^T W)\mathbf{s} \quad &\Rightarrow \quad \boldsymbol{f} \approx W\mathbf{s} = W(P^T W)^{-1} P^T \boldsymbol{f} \\
&\Rightarrow \quad \boldsymbol{f}_r(\boldsymbol{u}_r) = \boldsymbol{\Psi}^T \boldsymbol{f} \approx Q\tilde{\boldsymbol{f}}
\end{aligned}
$$

Approximating the nonlinearity

After finding P and $\wp = [\wp_1, \ldots, \wp_m]^T$

$$P^T \boldsymbol{f} = (P^T W)\mathbf{s} \quad \Rightarrow \quad \boldsymbol{f} \approx W\mathbf{s} = W(P^T W)^{-1} P^T \boldsymbol{f}$$
$$\Rightarrow \quad \boldsymbol{f}_r(\boldsymbol{u}_r) = \boldsymbol{\Psi}^T \boldsymbol{f} \approx Q\tilde{\boldsymbol{f}}$$

where

$$Q = \underbrace{\left(\boldsymbol{\Psi}^T W \underbrace{(P^T W)}_{m \times m}{}^{-1}\right)}_{N \times m \text{ (Precomputable)}}, \quad \tilde{\boldsymbol{f}} = \underbrace{P^T \boldsymbol{f}(\boldsymbol{\Psi} \boldsymbol{u}_r(t))}_{m \times 1}$$

A priori error bound

DEIM approximation satisfies the a priori error bound

$$\|\boldsymbol{f} - W(P^T W)^{-1}\boldsymbol{f}\|_2 \leq \|(P^T W)^{-1}\|_2 \|(I - WW^T)\boldsymbol{f}\|_2,$$

where the term $\|(P^T W)^{-1}\|_2$ is of moderate size of order 100 or less.

H. Antil, M. Heinkenschloss, and D. C. Sorensen, Application of the Discrete Empirical Interpolation Method to Reduced Order Modeling of Nonlinear and Parametric Systems , *A. Quarteroni and G. Rozzas (eds.), Reduced Order Methods for Modeling and Computational Reduction, Model. Simul.& Appl. Vol. 9, 2014, pp. 101–136,*

Degrees of freedoms with linear dG basis

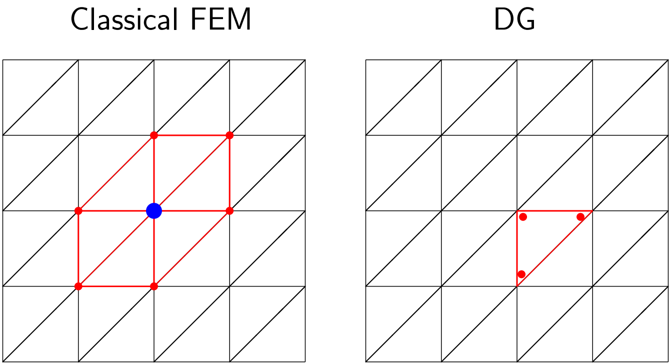

H. Antil, M. Heinkenschloss, and D. C. Sorensen, *Application of the Discrete Empirical Interpolation Method to Reduced Order Modeling of Nonlinear and Parametric Systems* , A. Quarteroni and G. Rozzas (eds.), Reduced Order Methods for Modeling and Computational Reduction, Model. Simul.& Appl. Vol. 9, 2014, pp. 101–136, Springer Italia, Milan.

Reduced Jacobian evaluation

The reduced Jacobian arising from DEIM

$$\frac{\partial}{\partial \boldsymbol{u}_r} \boldsymbol{f}_r(\Psi \boldsymbol{u}_r) \approx Q(P^T J_{\boldsymbol{f}})\Psi.$$

For $m = 4$, $\wp_2 = 6$ and $\wp_3 = 2$, and linear basis are used ($N_{loc} = 3$):

$$P^T \boldsymbol{f} = \begin{bmatrix} 0 & \dots & \dots & 1 & \dots & 0 \\ 0 & \dots & 1 & \dots & \dots & 0 \\ 0 & 1 & \dots & \dots & \dots & 0 \\ 0 & \dots & 0 & \dots & 1 & 0 \end{bmatrix} \begin{bmatrix} \boldsymbol{f}_1 \\ \vdots \\ \boldsymbol{f}_N \end{bmatrix} = \begin{bmatrix} \boldsymbol{f}_{\wp_1} \\ \boldsymbol{f}_6 \\ \boldsymbol{f}_2 \\ \boldsymbol{f}_{\wp_4} \end{bmatrix},$$

$$P^T J_{\boldsymbol{f}} = \begin{bmatrix} \dots & \dots & \dots & \dots & \dots & \dots & \dots & \dots \\ 0 & \dots & \frac{\partial \boldsymbol{f}_6}{\partial u_4} & \frac{\partial \boldsymbol{f}_6}{\partial u_5} & \frac{\partial \boldsymbol{f}_6}{\partial u_6} & 0 & \dots & 0 \\ \frac{\partial \boldsymbol{f}_2}{\partial u_1} & \frac{\partial \boldsymbol{f}_2}{\partial u_2} & \frac{\partial \boldsymbol{f}_2}{\partial u_3} & 0 & \dots & \dots & \dots & 0 \\ \dots & \dots & \dots & \dots & \dots & \dots & \dots & \dots \end{bmatrix},$$

Dynamic mode decomposition

- Equation-free, snapshot based method.
- Arnoldi-like algorithm based on the Koopman analysis.
- Modes and eigenvalues represents the temporal dynamics inherent in the data with oscillatory components.
- The modes are not necessarily orthogonal.
- DMD modes have a single-frequency content contrary to the POD modes that possess multi temporal frequency.

Optimality in POD	Optimality in DMD
$\Downarrow$	$\Downarrow$
Energy Criteria	**?**

B. O. Koopman. Hamiltonian systems and transformation in Hilbert space. Proceedings of the National Academy of Sciences, 17(5):315–318, 1931

- For the dynamic system specified by

$$x_{k+1} = g(x_k)$$

on a manifold $\mathscr{M}$, the Koopman operator maps any function $f : \mathscr{M} \to \mathbb{R}$ into

$$Af(x_k) = f(g(x_k)).$$

Koopman operator $A \to$ linear, infinite dimensional operator

- The function $f(x_k)$ can then be expressed as:

$$f(x_k) = \sum_{j=1}^{\infty} \alpha_j(x_0)\phi_j e^{(\omega_j + i\sigma_j)k},$$

ϕ_j:Koopman modes, w_j: growth rates and σ_j: frequencies of eigenvalues of A.

Dynamic mode decomposition method approximates the Koopman operator with a finite dimensional linear operator.

- **Snapshot matrix:** $\mathscr{S} = [\mathbf{u}^1, \ldots, \mathbf{u}^J]$ in $\mathbb{R}^{\mathscr{N} \times J}$ with

$$\mathscr{S}_0 = [\mathbf{u}^1, \ldots, \mathbf{u}^{J-1}], \quad \mathscr{S}_1 = [\mathbf{u}^2, \ldots, \mathbf{u}^J].$$

- Assume that $\tilde{\mathscr{A}} \in \mathbb{R}^{\mathscr{N} \times \mathscr{N}}$ a linear operator with

$$\mathscr{S}_1 \approx \tilde{\mathscr{A}} \mathscr{S}_0,$$

such that $\tilde{\mathscr{A}}$ minimizes the Frobenious norm

$$\|\mathscr{S}_1 - \tilde{\mathscr{A}} \mathscr{S}_0\|_F.$$

Problem: When N is large, it is hard to compute the matrix $\tilde{\mathscr{A}}$.

- **SVD of $\mathscr{S}_0$ with rank$(\mathscr{S}_0) = k$:**

$$\mathscr{S}_0 = U\Sigma V,$$

where, $U \in \mathbb{R}^{\mathscr{N} \times k}$ and $V \in \mathbb{R}^{J-1 \times k}$ are orthogonal matrices, $\Sigma \in \mathbb{R}^{k \times k}$ is the diagonal matrix.

- **POD projection of A :**

$$\begin{aligned} \tilde{A} &= U^* A U = U^* \mathscr{S}_1 (U\Sigma V^*)^{-1} U, \\ &= U^* \mathscr{S}_1 V \Sigma^{-1}. \end{aligned}$$

where $\tilde{A} \in \mathbb{R}^{k \times k}$ with $k < \mathscr{N}$.

- **Eigenvectors of A:**

$$\Phi^{\text{DMD}} = \mathscr{S}_1 \Sigma^{-1} V W,$$

where W is the eigenvector of $\tilde{A}$.

$\Phi^{\text{DMD}} \Longrightarrow$ DMD modes.

Exact DMD

Algorithm 2 Exact DMD Algorithm

Input: Snapshots $\mathscr{S} = [\mathbf{u}^1, \ldots, \mathbf{u}^J]$ with $\mathbf{u}^\mathbf{i} = \mathbf{u}_{t_i}$.
Output: DMD modes Φ^{DMD}.

1: Define the matrices $\mathscr{S}_0 = [\boldsymbol{u}^1, \ldots, \boldsymbol{u}^{J-1}]$ and $\mathscr{S}_1 = [\boldsymbol{u}^2, \ldots, \boldsymbol{u}^J]$.
2: SVD of $\mathscr{S}_0$: $\mathscr{S}_0 = \boldsymbol{U}\boldsymbol{\Sigma}\boldsymbol{V}^*$.
3: $\tilde{A} = \boldsymbol{U}^* \mathscr{S}_1 \Sigma^{-1} \boldsymbol{V}$.
4: Eigenvalues and eigenvectors of $\tilde{A}W = \Lambda W$
5: $\Phi^{\text{DMD}} = \mathscr{S}_1 \boldsymbol{\Sigma}^{-1} \boldsymbol{V} W$.

J. H. Tu, C. W. Rowley, D. M. Luchtenburg, S. L. Brunton, J. N. Kutz. On dynamic mode decomposition: theory and applications. J. Comput. Dyn., 1(2):391–421, 2014

- Equivalently,

$$\mathscr{S} = [\mathbf{u}^1, \ldots, \mathbf{u}^J] \approx \Phi^{\mathsf{DMD}} D_\alpha V_{\mathsf{and}},$$

$$D_\alpha = \begin{pmatrix} \alpha_1 & & & & \\ & \alpha_2 & & & \\ & & \ddots & & \\ & & & \alpha_{k-1} & \\ & & & & \alpha_k \end{pmatrix}, V_{\mathsf{and}} = \begin{pmatrix} 1 & \gamma_1 & & \gamma_1^{J-1} \\ 1 & \gamma_2 & & \gamma_2^{J-1} \\ & & \ddots & \\ 1 & \gamma_{k-1} & & \gamma_{k-1}^{J-1} \\ 1 & \gamma_k & & \gamma_k^{J-1} \end{pmatrix}$$

where $\gamma_i = \exp(\omega_i t)$, $i = 1, 2, \ldots, k$.

Optimal mode amplitudes

Aim: To identify the optimal mode amplitudes $\alpha = [\alpha_1(0), \ldots, \alpha_k(0)]$ with respect to the minimization problem:

$$\min_{\alpha} \|\mathscr{S} - \Phi^{\text{DMD}} D_\alpha V_{\text{and}}\|_F^2.$$

- Let $P = (W^*W) \circ (\overline{V_{\text{and}} V_{\text{and}}^*})$, $q = \overline{\text{diag}(V_{\text{and}} V \Sigma^* W)}$. where * denotes the conjugate transpose, $\circ$ denotes the elementwise multiplication.
- Then, $\alpha_{\text{opt}} = P^{-1} q$.

M. R. Jovanovič, P. J. Schmid, J. W. Nichols, Physics of Fluids 26, 024103, 2014

DMD approximation of the nonlinearity

Reduced approximation of the nonlinearity in terms of DMD modes

$$\tilde{\boldsymbol{f}}(t, \boldsymbol{u}) \approx \Phi^{\text{DMD}}(\mathrm{d}iag(e^{\omega^{DMD} t})\boldsymbol{b}$$

POD-DMD reduced system

$$\begin{aligned} \boldsymbol{M}_r \boldsymbol{u}_r &= -\boldsymbol{A}_r \boldsymbol{u}_r - (\Phi^{\text{POD}})^T \Phi^{\text{DMD}} \mathrm{d}iag(e^{\omega^{DMD} t})\boldsymbol{b} \\ \boldsymbol{u}(0) &= u_0^r \end{aligned}$$

$\boldsymbol{b} = \Phi^{\dagger} \boldsymbol{f}^1$
$\Phi^{\dagger}$: Moore-Penrose pseudo inverse of Φ^{DMD}.

Alessandro Alla and J. Nathan Kutz. Nonlinear model order reduction via dynamic mode decomposition.

arXiv:1602.05080, 2016.

2D Allen-Cahn equation with quartic potential

$$u_t = \varepsilon \Delta u + f(u)$$

Cubic bi-stable nonlinearity $f(u) = u^3 - u$

Homogenous Neumann boundary conditions

$\Omega = [0, 0.1]^2 \times [0, 0.025]$, $\Delta t = 0.00001$, $\Delta x = 0.003$

initial condition

$$u(x,0) = \tanh[(0.25 - \sqrt{(x_1 - 0.5)^2 + (x_2 - 0.5)^2})/(\sqrt{2}\varepsilon]$$

Parameter $\varepsilon = 0.02$

Allen, M.S., Cahn, J.W.: A microscopic theory for antiphase boundary motion and its application to antiphase domain coarsening. Acta Metallurgica 27(6), 1085–1095, 1979

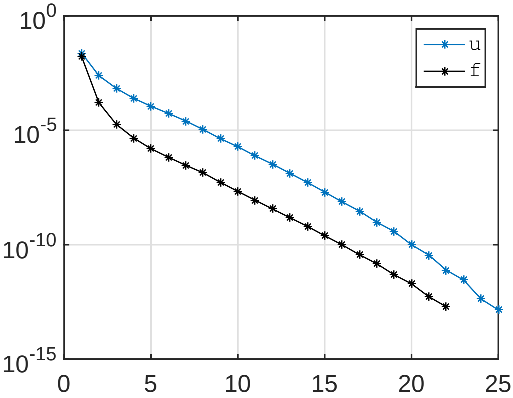

Figure 1: Decay of the singular values for u and the nonlinearity f.

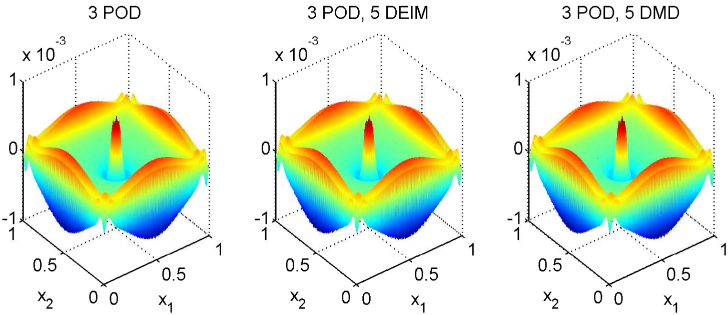

Figure 2: Plots of errors between FOM and ROM solutions

Comparison POD-DEIM-DMD

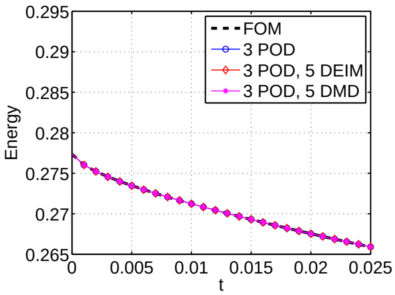

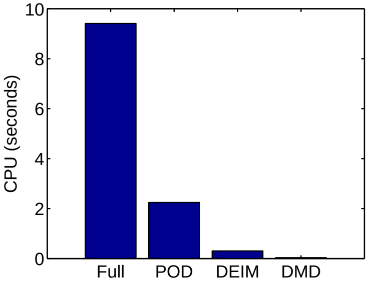

Figure 3: Energy plots (left) and CPU times (right)

Table 1: Energy errors between FOM and ROMs, and Speed-Up Factors

ROM	# Modes	Energy-Error	Speed-Up Factor
POD	3	1.97e-05	5.00
DEIM	5	1.96e-05	37.31
DMD	5	1.96e-05	416.86

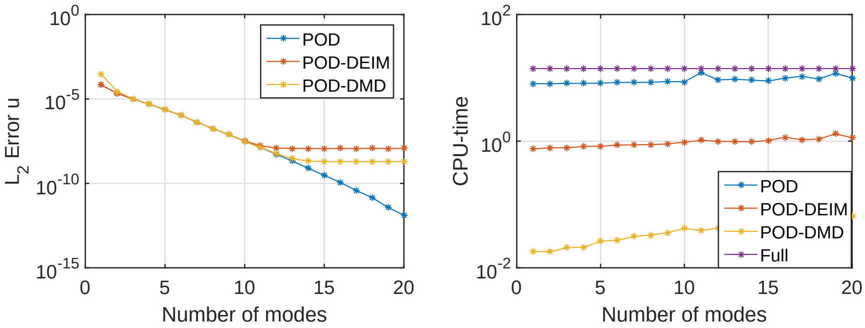

Figure 4: $L_2 - L_2$ FOM-ROM (left) and CPU times (right) with the same increasing number of POD, DEIM and DMD basis functions.

Diffusive FHN

$$
\begin{aligned}
u_t &= d_1 \Delta u - u^3 + u - v + \kappa, \\
v_t &= d_2 \Delta v - v + u
\end{aligned}
$$

space-time domain $Q = [-1,1]^2 \times [0,100]$.

Random initial conditions between -1 and 1 and zero flux boundary conditions

$\Delta x = \Delta y = 0.03125$ and temporal step-size $\Delta t = 0.1$.

Parameters $d_1 = 0.00028$, $\quad d_2 = 0.005$, $\quad \kappa = 0$

TT Marquez-Lago, P. Padilla, A selection criterion for patterns in reaction–diffusion systems. Theoretical Biology and Medical Modelling 11:7, 20167, 2014

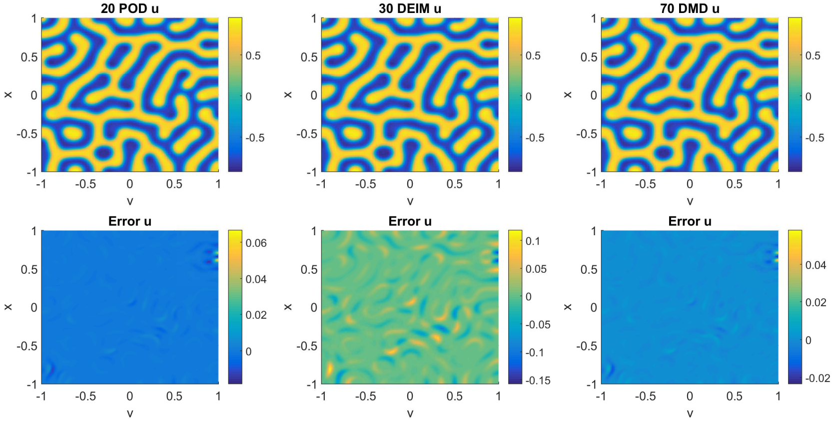

Figure 5: Labyrinthic patterns at $T = 100$ for POD, DEIM, DMD

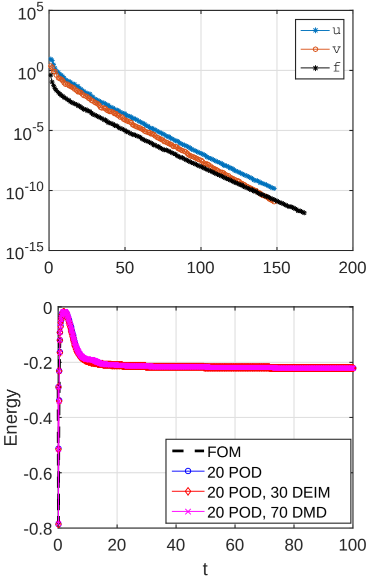

Figure 6: Decay of the singular values (upper), energy (lower)

ROM	#POD	#DEIM	#DMD	L_2-Error u	L_2-Error v	Speed-up
POD	20	-	-	1.81e-2	8.95e-3	1.73
DEIM	20	30	-	1.72e-1	4.49e-2	14.11
DMD	20	-	70	3.78e-1	1.00e-1	173.10

Table 2: FOM-ROM errors & speed-up

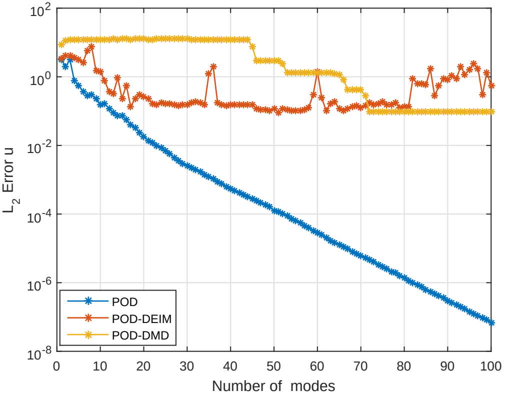

Figure 7: $L_2 - L_2$ FOM-ROM errors

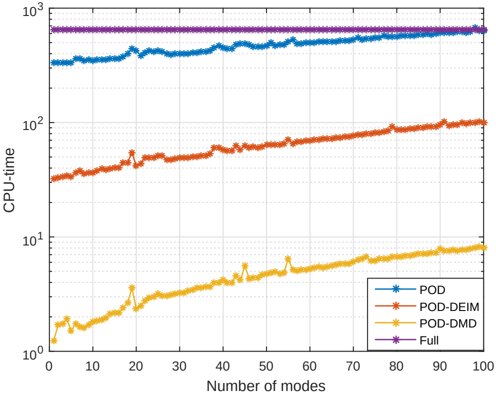

Figure 8: CPU times

Convective FHN

$$u_t = d_1 \Delta u - \mathbf{V} \cdot \nabla u - c_1 u(u - c_2)(u-1) - v,$$
$$v_t = d_2 \Delta v - \mathbf{V} \cdot \nabla v - \varepsilon(v - c_3 u)$$

On th space time cylinder $Q = \Omega \times (0,1)$, where $\Omega = (0,L) \times (0,H)$.

For a given $V_{max} = \frac{1}{4} a H^2$, the velocity field $V(y) = ay(H-y)$

Space-time domain $Q = \Omega \times [0,T] = [-1,1]^2 \times [0,100]$.

Random initial conditions between -1 and 1 and zero flux boundary conditions.

$\Delta x = \Delta y = 0.03125$ and temporal step-size $\Delta t = 0.1$.

Parameters $d_1 = 0.00028$, $d_2 = 0.005$, $\kappa = 0$

E. A. Ermakova, E. E. Shnol, M. A. Panteleev, A. A. Butylin, V. Volpert, F. I. Ataullakhanov. On propagation of excitation waves in moving media: The FitzHugh-Nagumo model. PLosOne, 4(2):E4454, 2009

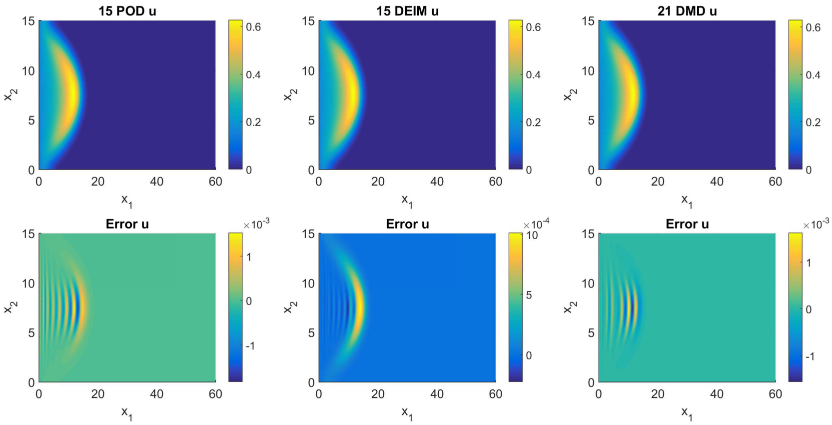

Figure 9: Standing waves at $T = 100$, POD, DEIM, DMD

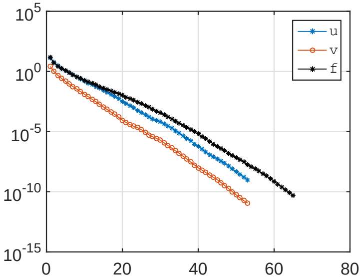

Figure 10: Decay of the singular values

ROM	#POD	#DEIM	#DMD	L_2Error u	L_2Error v	Speed-up
POD	15	-	-	2.48e-3	9.48e-5	1.41
DEIM	15	15	-	1.95e-3	2.68e-4	51.62
DMD	15	-	21	6.30e-3	3.02e-4	730.80

Table 3: FOM-ROM errors & speed-up

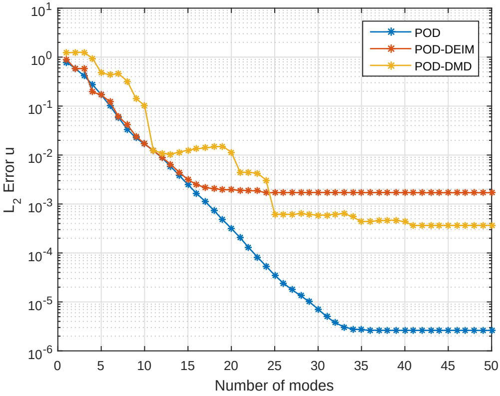

Figure 11: $L_2 - L_2$ FOM-ROM errors

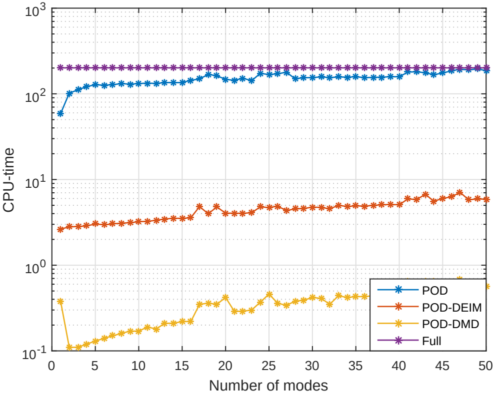

Figure 12: CPU times

Nonlinear Schrödinger

$$iu_t + \Delta u + 2|u|^2 u = 0 \text{ in } [0, 2\pi]^2 \times (0, 1]$$

with periodic boundary conditions and with the exact solution

$$u(x, y, t) = A \exp(i(c_1 x + c_2 y - \omega t))$$

$\omega = c_1^2 + c_2^2 - c|A|^2$. $A = c_1 = c_2 = 1$.

temporal and spatial mesh sizes
$\Delta t = 0.01$, $\Delta x = \Delta y = \pi/16 \approx 0.2$

Yan Xu and Chi-Wang Shu. Local discontinuous Galerkin methods for nonlinear Schrödinger equations. Journal of Computational Physics, 205(1):72–97, 2005

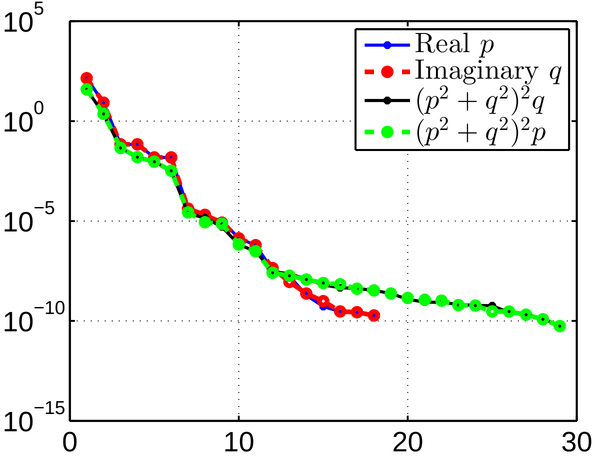

Figure 13: Singular values for the solutions and nonlinearities

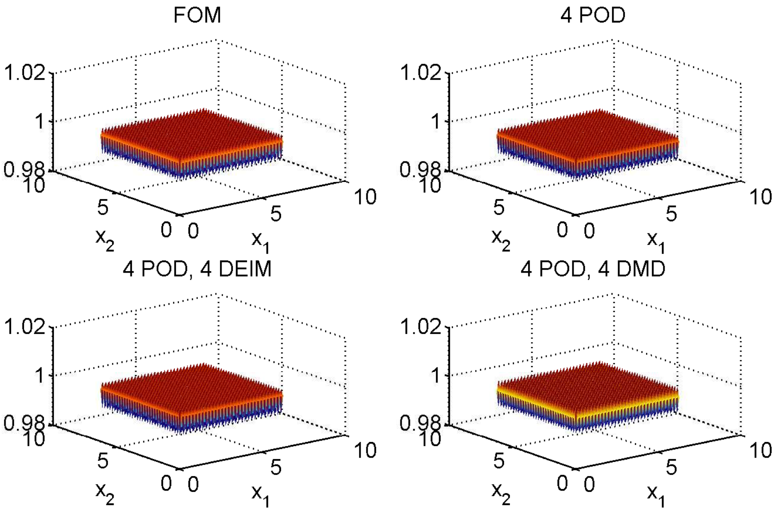

Figure 14: Solution profiles at the final time T =10

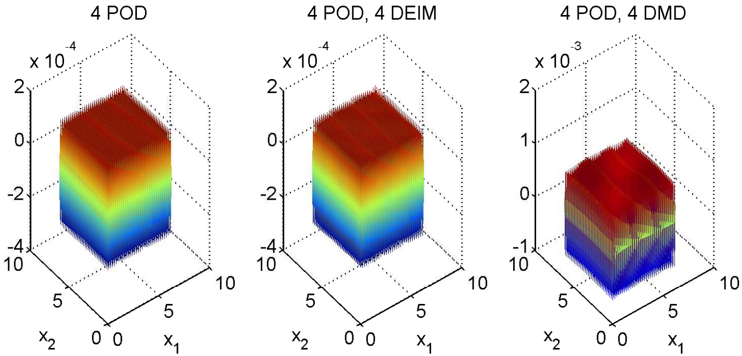

Figure 15: FOM-ROM errors at the final time

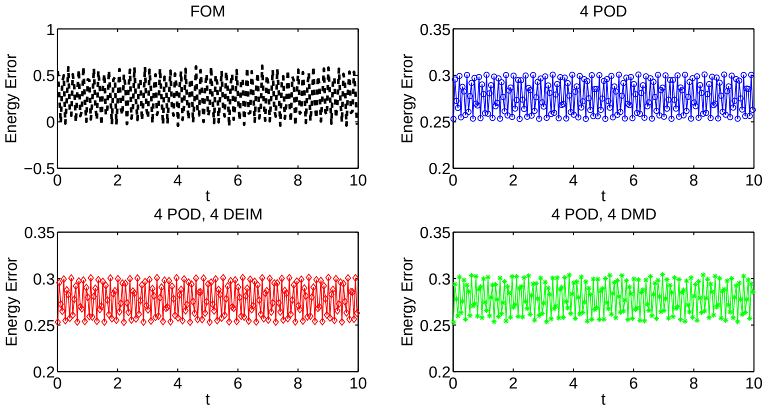

Figure 16: Energy errors $\int_\Omega -|\nabla u|^2 + |u|^4 d\Omega$

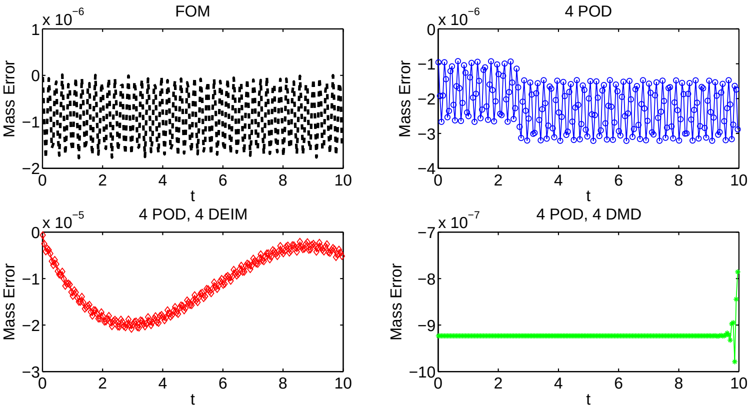

Figure 17: Mass errors $\int_\Omega |u|^2 d\Omega$

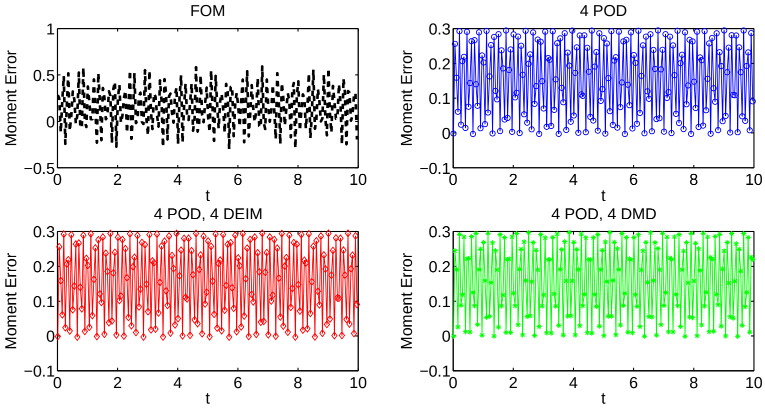

Figure 18: Momentum errors $\int \frac{1}{2}((uu^*{}_x - u^*u_x)) + (uu^*{}_y - u^*u_y))$

Table 4: The computation time (in sec) and speed-up factors

	FOM	POD	DEIM	DMD
CPU	1745.2	974.9	114.4	0.4
Speed Up		1.8	15.3	4085.9

Table 5: Errors between FOM

	Solution	Energy	Mass	Moment
POD	2.16e-03	7.75e-03	2.48e-08	3.83e-03
POD-DEIM	2.17e-03	7.75e-03	4.89e-07	3.83e-03
POD-DMD	1.94e-02	8.80e-03	2.62e-08	7.52e-03

Koopman operator

Discrete time dynamical system

$$\mathbf{x}_{k+1} = \mathbf{F}_f(\mathbf{x}_k)$$

Koopman operator on the observable function g

$$\mathcal{K}_t g(\mathbf{x}_k) = g(\mathbf{F}_t(\mathbf{x}_k)) = g(\mathbf{x}_{k+1})$$

System dynamics is characterized by

$$\mathcal{K} \varphi_k = \lambda \varphi_k$$

$$g(\mathbf{x}) = \begin{bmatrix} g_1(\mathbf{x}) & g_2(\mathbf{x}) & \cdots & g_p(\mathbf{x}) \end{bmatrix}^T = \sum_{k=1}^{\infty} \varphi_k(\mathbf{x})\mathbf{v}_k$$

$$\mathcal{K} g(\mathbf{x}) = \mathcal{K} \sum_{k=1}^{\infty} \varphi_k(\mathbf{x})\mathbf{v}_k = \sum_{k=1}^{\infty} \mathcal{K} \varphi_k(\mathbf{x})\mathbf{v}_k = \sum_{k=1}^{\infty} \lambda_k \varphi_k(\mathbf{x})\mathbf{v}_k$$

Observables

Observables $\mathbf{g}(\mathbf{x})$

mapping from the *physical space* to *feature space*

System dynamics is characterized in the feature space by

Koopman eigenvalues λ_k, eigenfunctions $\varphi_k(\mathbf{x})$, and modes $\mathbf{v}_k$

Construction of the feature space $\mathbf{g}(\mathbf{x})$

- Polynomials $g_j(x) = \{x, x^2, x^3, \ldots, x^n\}$
- Radial basis functions
- Hermite polynomials
- Discontinuous spectral elements

Column size of the data matrix n, number of snapshots m

Extended DMD when $n >> m$

Examples for observables for NLS

$$\mathbf{g}_1(\mathbf{x}) = \begin{bmatrix} \mathbf{x} \\ |\mathbf{x}|^2\mathbf{x} \end{bmatrix}, \quad \mathbf{g}_2(\mathbf{x}) = \begin{bmatrix} \mathbf{x} \\ |\mathbf{x}|^2 \end{bmatrix}$$

Kernel DMD $m >> n$, SVM based kernels

- polynomial kernel $f(\mathbf{x},\mathbf{x}') = (a + \mathbf{x}^T\mathbf{x}')^p$
- radial basis functions $f(\mathbf{x},\mathbf{x}') = exp(-a|\mathbf{x} - \mathbf{x}|^2)$
- sigmoid kernel $f(\mathbf{x},\mathbf{x}') = tanh(\mathbf{x}^T\mathbf{x}' + a)$

Perform DMD on the data matrices of the observables

J. Nathan Kutz and Steven L. Brunton, Dynamic Mode Decomposition: Data-Driven Modeling of Complex Systems, SIAM, 2016.

- From the foreword "Oberwolfach Mini-Workshop: Applied Koopmanism, 7– 13 February 2016
  "Poincaré suggested that complicated dynamics governed by non-linear partial differential equations can be reduced to and analyzed with the novel (at that time) linear infinite dimensional spectral methods advocated by Hilbert and Fredholm, ...Poincaré's vision became reality a good two decades later by landmark contributions of Carleman, Koopman and von Neumann."
- Prediction from the data as fourth paradigm of scientific discovery, "New Report on Research and Education in Computational Science and Engineering, September 2016"
- Data-Driven Methods for Reduced-Order Modeling and Stochastic Partial Differential Equations, Banff International Research Station University of British Columbia, January 29 - February 3, 2017.